

UNCLASSIFIED

2019
C121

35

Technical Memorandum

1 st Review Date: <u>6-18-81</u>		Determination (Circle Number):	
Authority: <input type="checkbox"/> ADCC <input checked="" type="checkbox"/> ADD	<u>CCRP RR</u>	Classification Review	<u>U</u>
Name:		1. Date of Review (DD-MY-YY)	
2 nd Review Date: <u>12-16-96</u>		2. Date of Review (DD-MY-YY)	
Authority: <u>W. L. ...</u>		3. Date of Review (DD-MY-YY)	
Name:		4. Date of Review (DD-MY-YY)	
		5. Date of Review (DD-MY-YY)	

SCTM- 235-55-51

ESTIMATES OF THE ACCURACY OF AN INDICATOR OF THE VERTICAL IN AN AIRPLANE

R. L. Calvert

ABSTRACT

Mathematical expressions for the errors in an indicator of the vertical in an airplane are derived and evaluations are discussed. Random errors due to atmospheric turbulence and predictable errors due to the earth's rotation, straight and level flight of the airplane, Coriolis acceleration, gyro drift, and some sustained airplane maneuvers are included.

Errors in indicated vertical (during flight through clear air) rarely will exceed a few tenths of a degree, if the corrections are made for predictable errors. If such corrections are not made, the error rarely will exceed one degree.

CLASSIFICATION CHANGED TO: <u>U</u>		AUTHORITY: <u>CCRP-RR</u>
PERSON CHANGING MARKING & DATE: <u>Emelda Selph</u>		RECORD ID: <u>973N148</u>
PERSON VERIFYING MARKING & DATE: <u>J. L. ...</u>		DATED: <u>12/17/96</u>

INVENTORIES
DATE: 2-22-89

Case No. 418.01

November 4, 1956

UNCLASSIFIED

DISTRIBUTION:

- S. C. Hight, 5100
- R. A. Bice, 5200
- E. F. Cox, 5110
- R. W. Shephard, 5120
- K. W. Erickson, 5130
- G. E. Hansche, 5140
- A. P. Gruer, 5210
- L. D. Smith, 1212
- J. W. Jones, 1214
- W. J. Denison, 1216
- D. R. Cotter, 1321
- R. H. Schultz, 1323
- A. W. Fite, 1324
- L. Gutierrez, 1331
- W. M. Wells, 1332
- W. E. Treible, 1335
- W. D. Wood, 5122
- S. H. Dike, 5123
- R. S. Claassen, 5133
- H. S. North, 5211
- A. E. Bentz, 5213
- C. F. Bild, 5311
- A. E. Winblad, 5321
- E. H. Copeland, 5351
- A. J. Clark, Jr., 5352
- J. P. Shoup, 5413
- C. H. Bidwell, 5441
- R. L. Calvert, 5131
- R. K. Smeltzer, 1922-2
- H. M. Willis, 1923 (6)



UNCLASSIFIED
TABLE OF CONTENTS

	Page
I. INTRODUCTION	4
II. DISCUSSION AND SUMMARY	5
Calibration of Double-Integrating Accelerometer	5
Advantage of Vertical Indicators	5
Vertical Indicator in Aircraft	6
Definitions	6
Some Predictable Effects	7
Need for Torque Cutout	8
Deviation Between Static Vertical and Dynamic Vertical	8
Deviation Between Static Vertical and Indicated Vertical	10
Conclusions	12
III. METHOD OF APPLYING TORQUES	13
IV. EFFECTS OF EARTH'S ROTATION, AIRPLANE'S STRAIGHT AND LEVEL FLIGHT, CORIOLIS ACCELERATION, GYRO DRIFT, AND AIRPLANE MANEUVERS ON INDICATED VERTICAL	16
Earth's Rotation and Straight and Level Flight	16
Coriolis Acceleration	18
Gyro Drift	19
Airplane Maneuvers	19
V. ESTIMATES OF DIFFERENCES BETWEEN STATIC AND DYNAMIC VERTICALS FOR SEVERAL AIRPLANES	22
Correlation of Gust Frequency with Altitude	22
Aircraft Motions Through Atmospheric Turbulence	23
Angular Differences Between Dynamic and Static Verticals	25
VI. ESTIMATES OF ERRORS IN INDICATED VERTICAL BECAUSE OF ATMOSPHERIC DISTURBANCES.	29
Method of Applying Torques	29
Mathematical Models	29
Errors in Indicated Vertical Because of Gusts	31
APPENDIXES	
A. FUNDAMENTALS OF GYROSCOPE THEORY	35
B. DIFFERENCE BETWEEN DYNAMIC VERTICAL AND STATIC VERTICAL IN AN AIRPLANE.	37
Coriolis Acceleration	40
LIST OF REFERENCES	42

UNCLASSIFIED

CHAPTER I

INTRODUCTION

This report is a study of the accuracy with which the true vertical (direction of the gravity vector) can be determined in an airplane in flight. This is one of a series of reports which consider various problems connected with the fuzing of weapons by distance measurement (vertical distance in particular). However, the value of this report is not restricted to its fuzing applications. For example, autopilots, bomb directors, fire-control mechanisms, and aerial mapping methods require vertical references.

The major problems involved in vertical-distance fuzing are (1) the determination of altitude with respect to desired burst height, (2) the accuracy of distance measurements with double-integrating accelerometers, and (3) the accuracy with which a vertical reference can be maintained.

The determination of the weapon-release altitude with respect to desired burst height has been considered in connection with time-of-fall fuzing of strategic weapons.¹

The accuracy of accelerometers for vertical distance measurement and the necessary calibrations have been discussed with considerable detail.²

The vertical reference problem can be divided into two parts. The first part deals with the accuracy of a vertical reference in the airplane for purposes of calibrating and initiating the fuzing device in the weapon before release. (This problem is discussed in this report.) The second part deals with the design and accuracy of the vertical reference carried by the weapon in free fall or in free flight.

Some preliminary comparisons of fuzing by means of distance measurement with other fuzing methods are found in Reference 3.

In Chapter II the results from the remainder of this report are collected and discussed.

CHAPTER II

DISCUSSION AND SUMMARY

Pertinent results from the remaining chapters of this report are summarized in this chapter along with the salient features of methods used in the analysis. For the benefit of the reader who may not wish to follow through the mathematics of later chapters, this discussion includes all results that are of interest. Therefore, there is considerable duplication between this chapter and those that follow.

Calibration of Double-Integrating Accelerometer

An earlier report² suggests a method for calibrating the double-integrating accelerometers for the vertical distance measurement. This calibration procedure requires a period of straight and level flight while the airplane is in the vicinity of the target. For the purpose of this report it is assumed that four minutes is sufficient time for this period of straight and level flight. The duration of this period of flight is of significance to this report mainly in estimating the probability of occurrence of certain errors in the indicated vertical. This report considers a system which would have a vertical indicator in the aircraft to serve as a reference for the stable platform which carries the accelerometers in the weapon. The first operation during the short calibration flight would be the aligning of the vertical indicator in the weapon with the vertical reference in the aircraft.

Advantages of Vertical Indicators

The use of vertical indicators in both aircraft and weapons appears to have certain advantages. Because the weapon is more or less unrestricted in its angular motions, a stable platform, not a single-gyro system, is required to carry the accelerometer. If the stable platform is expected to be used for only a short time, it can be comparatively simple in construction and not subject to stringent drift-rate requirements. Furthermore, if the run-down time of the gyros in the platform is sufficiently long, it might be possible to dispense with a gyro power supply. Because the airplane is somewhat restricted in its angular motions, a comparatively simple, one-gyro vertical indicator is sufficient for use in aligning the vertical in the weapon during the calibration run.

UNCLASSIFIED

Vertical Indicator in Aircraft

For the purpose of this analysis the vertical indicator in the aircraft consists of a two-degree-of-freedom gyro with a pendulum on gimbals so that the center of gravity of the gyro rotor is effectively the point of suspension of the pendulum. Torques are generated when the pendulum differs in direction from the gyro spin axis. Torques are applied in such fashion that the torque axis is in the plane defined by the pendulum and the gyro spin axis and perpendicular to the latter. Torques applied in this fashion erect the gyro directly toward the pendulum. Before the application of torques can be discussed further several definitions are required.

Definitions

The static (true) vertical is the direction of the gravity vector, \bar{g} . The dynamic vertical is the direction defined by the pendulum. If \bar{a} is the resultant of all accelerations other than \bar{g} acting at the center of gravity of the gyro rotor, then the direction of the resultant of \bar{g} and $-\bar{a}$ is the dynamic vertical. The gyro spin axis is the indicated vertical. The angle between indicated vertical and dynamic vertical is denoted by β . The angle between static vertical and dynamic vertical is denoted by ϵ . The angle between static and indicated vertical is denoted by γ . (See Fig. 1.)

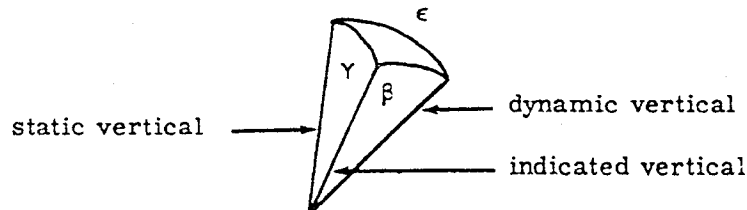


Fig. 1 -- General orientation of the three verticals.

Torques are applied in three regimes. In regime (a) the torque is proportional to β . Regime (a) is in operation when $0 < \beta \leq 2^\circ$. In regime (b) the torque is constant at its value when $\beta = 2^\circ$. Regime (b) is in operation when $2^\circ \leq \beta \leq 10^\circ$. Under regime (c), that is, when $10^\circ < \beta$, no torque is applied. Regime (c) prevents the accumulation of large errors in the indicated vertical during sustained maneuvers such as substantial changes in aircraft heading. The torques are defined completely when the gyro erection rate is specified in regime (b). In this report two erection rates are used: 2° per minute and 10° per minute. No feature is proposed in this analysis which is not already in use in gyro technology. However, the writer does not know whether all proposed features have been built into a single-gyro system.

Some Predictable Effects

A perfect gyro maintains its spin axis in a fixed direction in inertial space as long as no torques are applied. Such a gyro, if fixed on the earth, would indicate the vertical only at the geographic poles. In the system analyzed here the indicated vertical comes to rest at some value of β such that the torque generated by the system is sufficient to cancel the effects of the earth's rotation. (The static and dynamic verticals are coincident.) This error in the indicated vertical is latitude (λ) dependent. The error is $0.05^\circ \cos \lambda$ when the erection rate is 10° per minute in regime (b) or $0.25^\circ \cos \lambda$ when the erection rate is 2° per minute. In this situation the indicated vertical leans to the west of the static vertical.

Now consider the effect of unaccelerated straight and level flight of the aircraft carrying the vertical indicator over a nonrotating earth. Assume a speed of 1000 ft/sec. Under these conditions the vertical indicator is in error by 0.033° when the erection rate is 10° per minute in regime (b) or by 0.16° when the erection rate is 2° per minute. The error in the indicated vertical is toward the tail of the airplane. For speeds other than 1000 ft/sec the error is in the same proportion as the speeds.

Bearing friction in the gyro and in the gimbals generates torques which cause the gyro to drift and thus introduce another source of error in the indicated vertical. Drift rates as low as 1° per hour appear to be attainable with relative ease. Such a drift rate is balanced by a deviation between indicated vertical and dynamic vertical of 0.003° when the erection rate is 10° per minute in regime (b) and by 0.016° when the erection rate is 2° per minute. This error is considered negligible.

For an airplane flying straight and level at 1000 ft/sec Coriolis acceleration causes an error of $0.25^\circ \sin \lambda$ in the indicated vertical which leans in a direction 90° to the left of the aircraft heading (in north latitudes). For all realistic values of flight speed the error in indicated vertical is directly proportional to $0.25^\circ \sin \lambda$.

For errors in the indicated vertical caused by the earth's rotation, the airplane's 1000-ft/sec flight and Coriolis acceleration can combine to give a total error as large as 0.40° (approximately) when the slow erection rate is used. If the fast erection rate is used, the maximum total error in indicated vertical is approximately 0.28° for these three sources combined.

Need for Torque Cutout

Thus far the need for regime (c) has not been mentioned. This need is emphasized by sustained maneuvers such as a 180° perfectly banked turn. Suppose that regime (b) is in effect for all $\beta > 2^\circ$ (i.e., regime (c) is absent). Consider a perfectly banked turn through 180° at $2g$ and 500 ft/sec, or at $4g$ and 1000 ft/sec. At the end of such a turn the indicated vertical is in error by 4° when the faster erection rate is used and by 0.8° when the slower erection rate is in effect. After return to straight and level flight this error is reduced to 0.1° in 0.8 minute when the erection rate is 10° per minute in regime (b) or in 2 minutes when the erection rate is 2° per minute. This error is reduced to 0.01° after 1.2 minutes under the faster erection rate and after 4.4 minutes under the slower erection rate.

The examples of the preceding paragraph illustrate the need for regime (c). With regime (c) present the errors in the indicated vertical caused by the radial acceleration during the turn are negligible provided there is a direct transition between straight and level flight and the perfectly banked turn.

Next consider a turn at low radial accelerations. A 90° turn at $0.17g$ and 500 ft/sec requiring about 2.5 minutes illustrates the situation. (Such a maneuver may be expected of bombers in formation approaching a bombing run.) At the end of this maneuver the indicated vertical is approximately 10° in error when the gyro erects at 10° per minute in regime (b) or 5° in error when the gyro erects at 2° per minute. After the completion of the turn the error is reduced to 0.1° in 1.4 minutes and 4.5 minutes for the fast and slow erection rates, respectively. The times required to reduce the error to 0.01° are roughly one-fourth longer. From this example it appears advisable to provide a complete cutout so that no torque is applied during slow maneuvers.

Deviation Between Static Vertical and Dynamic Vertical

Chapter V applies the theory developed in Appendix B to determine the deviation, ϵ , between static vertical and dynamic vertical for airplanes passing through gusts. Aircraft used as examples are the B-36D, B-47B, B-52, F84F, and the F2H-2. Only one source of information was found which gave angular velocities and accelerations as well as linear accelerations for an airplane (B-45C) flying through gusts in clear air. These data are converted for use with the airplanes mentioned. Values of ϵ are computed for altitudes of

15,000 and 35,000 feet (25,000 feet for the B-36D) as well as for two positions in the aircraft -- the center of gravity and the nose.*

Several investigations of frequency and magnitude of gustiness in clear air serve as a basis for estimating the probability of occurrence of errors in the indicated vertical.

Lack of information on the life history of disturbances to straight and level flight makes certain assumptions necessary. In particular it is necessary to assume that maximum angular accelerations occur simultaneously with maximum linear accelerations. (Angular velocities of the aircraft play a minor role in the determination of ϵ .) Also, it is necessary to assume that all angular motions have the same period. These assumptions lead to values of ϵ larger than the correct values. (Maximum values of ϵ are denoted by ϵ_{max} .) These assumptions apply only to a vertical indicator not situated at the center of gravity of the aircraft.

For the purpose of estimating maximum errors in the indicated vertical three typical values of ϵ_{max} are chosen from the results of Chapter V: 2° , 7° , and 27° .

The 2° difference between static and dynamic verticals is typical of disturbances which will be exceeded with probability approximately one during the four-minute calibration flight. This value is typical of both fighter and bomber aircraft at both altitudes considered in this memorandum and with the vertical indicator at the center of gravity of the aircraft.

The value $\epsilon_{max} = 7^\circ$ is typical of disturbances expected rarely (with probability less than 0.04) with an instrument at the center of gravity of the aircraft except for the fighters at the 15,000-foot altitude. This value of ϵ_{max} is also typical of disturbances to be expected with probability approximately one during a four-minute calibration run with the instrument in the nose of the aircraft.

The value $\epsilon_{max} = 27^\circ$ is typical of differences between static and dynamic verticals to be exceeded rarely (with probability approximately 0.04) during the calibration run when the vertical indicator is in the nose of the aircraft. Actually values of ϵ_{max} twice as large are

* Flexure of the airplane may introduce large initial errors in the indicated vertical in the weapon if the weapon vertical is aligned with the indicated vertical in the aircraft, some distance away from the bomb bay. This problem is not considered here.

computed for the F-84F and the F2H-2 at the 15,000-foot altitude. However, regime (c) is in operation throughout the greater part of disturbances of such magnitude. Hence such large values of ϵ_{\max} do not contribute the largest errors in the indicated vertical.

Deviation Between Static Vertical and Indicated Vertical

In Chapter VI estimates of γ , the deviations between static and indicated verticals, are derived. These values of γ correspond to the values of ϵ_{\max} discussed in the preceding paragraphs.

Because the timewise history of aircraft motions induced by gusts is not known, it is necessary to assume that the three verticals are coplanar during the disturbance. In addition, it is necessary to bracket the variations in ϵ by expressing ϵ in terms of a sine function in one situation and as a heavily damped sine function in the other. Figures 3 and 4 at the end of Chapter VI illustrate the variation in both ϵ and γ for both functional representations.

Periods of variation in the motion of aircraft lie between two and ten seconds. For the purpose of this study it is assumed that ϵ varies with the same period. Because the error in the indicated vertical (generated by passing through a gust) increases with the period, a ten-second period is used for illustration (Figs. 3 and 4, pp 32 and 33). This choice leads to conservative estimates of errors in the indicated vertical. For a period of five seconds in the variation of ϵ the errors in indicated vertical are nearly 50 per cent smaller than for a ten-second period.

As should be expected the largest values of γ , the error in the indicated vertical, occur when regime (b) is in operation throughout most of the cycle of variation in ϵ .

When $\epsilon_{\max} = 2^\circ$ or 7° and ϵ has a ten-second period, the maximum value of γ is approximately 0.4° or 0.7° , respectively. This statement applies to either the sine function variation in ϵ or the damped sine function. When $\epsilon_{\max} = 27^\circ$, the sine function gives a maximum value of $\gamma = 0.2^\circ$ and the damped sine function gives a maximum $\gamma = 0.5^\circ$. These values of γ are based on a gyro erection rate of 10° per minute in regime (b). If the gyro is erected toward the dynamic vertical at 2° per minute, the maximum value of γ is 0.2° when $\epsilon_{\max} = 7^\circ$, and 0.1° when $\epsilon_{\max} = 2^\circ$ or 27° .

The direction and magnitude of the resultant error in indicated vertical because of the earth's rotation, the linear motion of the aircraft, and Coriolis acceleration depend on airplane speed, course, and latitude. The direction of the error in indicated vertical because of clear air gusts is unknown for an instrument in the nose of the airplane; for an instrument at the airplane center of gravity the direction is 90° from the flight path (right or left). Therefore, it is difficult to combine errors arising from these sources. However, it is possible to obtain some maximum values.

Consider the situation in which the gyro erection rate is 10° per minute in regime (b) and the indicated vertical is at the center of gravity of the airplane. The error in the indicated vertical because of a gust rarely will exceed 0.7° . The other errors in the indicated vertical will combine to equal 0.28° only when the airplane is at 45° latitude with the proper heading. Hence, the indicated vertical will rarely be in error by as much as 1° . The preceding statement is based on a 1000-ft/sec flight speed and a ten-second period for ϵ . (If ϵ varies with a five-second period, this extreme value is reduced to 0.7° .)

If the 2° -per-minute erection rate is used, the indicated vertical rarely would be in error by as much as 0.6° when the period of ϵ is ten seconds and slightly less when the period is five seconds. In this situation, only 0.2° of the error would be contributed by gustiness. Therefore, it is feasible to maintain a vertical indicator within 0.2° of true vertical provided extra computers and torquers can be added to the system analyzed here so as to cancel the errors arising from the earth's rotation, the airplane's straight and level flight, and the Coriolis acceleration.

The extremes of 1° and 0.6° noted in the two preceding paragraphs are reduced approximately 0.1° by reducing the air speed to 500 ft/sec.

When $\epsilon_{\max} = 2^\circ$ it is possible for errors in the indicated vertical to combine in a value between 0 and 0.1° . Therefore zero is the lower limit for errors in the indicated vertical during the calibration run. Obviously such a lower limit is not particularly useful. Latitude and course angle would need be specified before a more useful lower limit could be found which then would apply to, at most, a few particular situations.

Consider the situation in which the vertical indicator is in the nose of the aircraft, the erection rate of the gyro is 10° per minute, and ϵ has a ten-second period. Then the indicated vertical is almost certain to be in error by at least 0.3° during the calibration run.

UNCLASSIFIED

Because of the operation of regime (c) the error rarely will exceed 1.2° (approximately) under the conditions of this analysis. If the five-second period is used for ϵ , these extreme values both are 0.3° smaller.

Errors in the vertical at high altitudes caused by the earth's physical irregularities are generally less than one minute of arc.⁴ For the purpose of this analysis such errors are negligible.

A short discussion of errors in burst height caused by errors in the vertical indicator is given in Reference 2. An example given in that reference indicates that such errors rarely will be as large as 300 feet.

Conclusions

The significant conclusions to be drawn from this report follow.

1. A vertical indicator located at the center of gravity of the airplane and consisting of a two-degree-of-freedom gyro with torques applied by a pendulum through resolvers rarely will be in error by as much as 1° on a straight and level calibration run of four minutes through clear air.
2. Errors in the indicated vertical can be reduced to a few tenths of a degree if additional computers and torquers are provided to cancel the effects of the earth's rotation, the airplane's straight and level flight, and Coriolis acceleration.
3. More accurate estimates of errors in the vertical indicator cannot be made until much more information is available concerning the accelerations acting on an airplane under atmospheric conditions more representative of actual use of a vertical-distance fuze.

UNCLASSIFIED

CHAPTER III

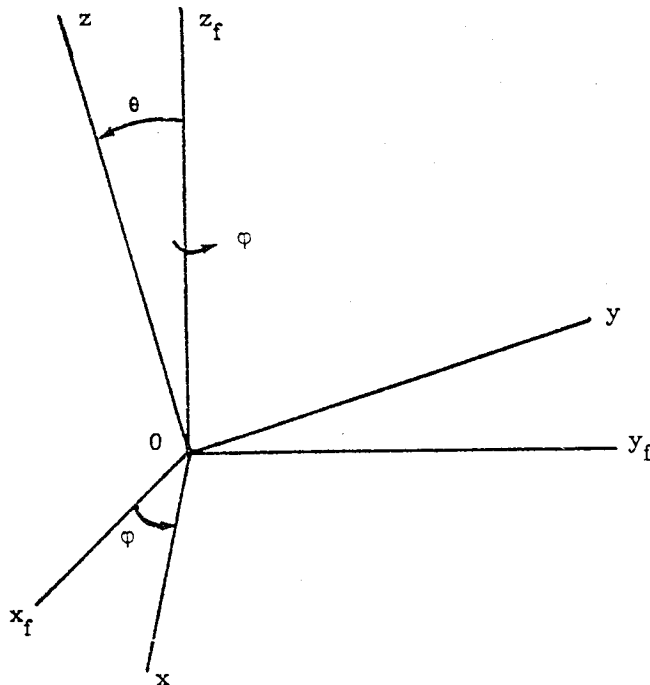
METHOD OF APPLYING TORQUES

A gyro tends to maintain its spin axis with a direction fixed in inertial space. Therefore, it is necessary to apply certain torques to convert the gyro into an effective indicator of the vertical. These torques are discussed in later chapters of this report as they apply to specific situations. The method of applying these torques is discussed in the following paragraphs.

In Appendix A the following equations are derived:

$$\left. \begin{aligned} L_x &= I_z s \dot{\varphi} \sin \theta, \\ L_y &= -I_z s \dot{\theta}, \\ L_z &= 0. \end{aligned} \right\} \quad (1)$$

These equations relate the components of torque, L , and the motions of the gyroscope, $\dot{\varphi}$ and $\dot{\theta}$. I_z is the moment of inertia of the gyro rotor about its spin axis; s is the constant spin velocity of the gyro rotor. Equations 1 apply when the gyro coordinate system, 0 - x y z , is defined as in Fig. 2. (0 - x_f y_f z_f is an arbitrary inertial coordinate system.)



O is the center of gravity of the gyro rotor. Oz is the gyro spin axis. Oy is in the Ozz_f plane. Ox is in the $Ox_f y_f$ plane.

Fig. 2 -- Two rectangular coordinate systems.

UNCLASSIFIED



In this analysis it is assumed that torques are applied so that $\dot{\phi}$ (and therefore L_x also) is zero. Therefore, subscripts are dropped and Equations 1 become

$$L = -I_z s \dot{\theta}. \tag{2}$$

When Equation 2 is applied it is important to remember that the torque axis is perpendicular to the gyro spin axis and in the plane determined by the spin axis and the position (line) which it is desired that the spin axis take. This latter position lies between the positive spin axis and the positive torque axis.

Special forms for Equation 2 are discussed in later paragraphs of this chapter. Specific applications are made in later chapters. Special coordinate systems required in discussing the applications are defined as they are needed.

Insofar as possible it is advisable to apply torques in such a manner that errors in their computation or application do not accumulate with time and thus destroy the effectiveness of the gyro as an indicator of the vertical. In this analysis it is generally assumed that the required torques are activated by a pendulum which controls the action of the gyro through the necessary resolvers and servomechanisms. The pendulum is effectively suspended from the center of gravity of the gyro. The gyro itself is not pendulous.

The pendulum will sense the true or static vertical (the direction of the gravity vector) only when no accelerations other than gravity are acting on the instrument. If \bar{a} represents the resultant of all accelerations other than that of gravity, \bar{g} , acting on the center of gravity of the gyro, the pendulum aligns itself with the resultant of $-\bar{a}$ and \bar{g} . The resultant of $-\bar{a}$ and \bar{g} is defined to be the dynamic vertical.

The dynamic vertical coincides with the static vertical only when no acceleration other than that of gravity is acting. However, the deviations from straight and level flight of the airplane are approximately normally distributed about a zero mean. Therefore, in flight through clear air, the average position of the dynamic vertical will approximate the static vertical. A difference in direction between the gyro spin axis and the dynamic vertical activates a torque which moves the gyro spin axis (indicated vertical) toward the dynamic vertical. Because the motion of the gyro spin axis lags behind that of the dynamic vertical, the spin axis presents a smoothed or averaged indication of the vertical. Hence, in general, the indicated vertical will differ less from its average position than does the dynamic vertical. A quantitative discussion of this method of applying torques is contained in the following paragraphs.



The only torques which are active along the spin axis are those required to maintain a constant spin velocity. These torques will be supplied independently of the scheme discussed in the preceding paragraphs and will not be discussed further. All other torques (i. e., those which produce gyro motion other than spin) will have $L_z = 0$.

Let γ be the angle between static and indicated verticals, ϵ be the angle between static and dynamic verticals, and β be the angle between indicated and dynamic verticals. (See Fig. 1 page 6.) No simple relation exists between γ , ϵ , and β . However,

$$|\epsilon - \gamma| \leq \beta \leq \epsilon + \gamma,$$

where negative values of the angles are not defined.

A torque is activated when $\beta \neq 0$. Assume that the torque is applied so that its axis is perpendicular to the indicated vertical (gyro spin axis) and in the plane determined by the dynamic and the indicated verticals. Then, if the torque has the proper sign, the precession of the indicated vertical is directly toward the dynamic vertical.

Torques L are applied to the gyro under three regimes:

$$\left. \begin{array}{ll} \text{(a)} & L = I_z s K \beta \frac{\pi}{180} \text{ for } 0 \leq \beta \leq \beta_1, \\ \text{(b)} & L = I_z s K \beta_1 \frac{\pi}{180} \text{ for } \beta_1 \leq \beta \leq \beta_2, \text{ and} \\ \text{(c)} & L = 0 \text{ for } \beta_2 < \beta \end{array} \right\} \quad (3)$$

where K , β_1 , and β_2 are constants, $\beta_1 = 2^\circ$, and $\beta_2 = 10^\circ$. Two values, $1/12$ and $1/60$, are used for K . Values of $1/12$ and $1/60$ for K correspond to gyro response rates of $1/6$ and $1/30$ degree per second (10° and 2° per minute), respectively. (The factor $\pi/180$ converts degrees to radians.) Because torques are applied so as to reduce β , the negative sign of Equation 2 is dropped.

Application of Equations 2 and 3 to situations arising from the earth's rotation, the airplane's straight and level flight, some simple airplane maneuvers, and gyro drift are made in Chapter IV.

CHAPTER IV

EFFECTS OF EARTH'S ROTATION, AIRPLANE'S STRAIGHT AND LEVEL FLIGHT, CORIOLIS ACCELERATION, GYRO DRIFT, AND AIRPLANE MANEUVERS ON INDICATED VERTICAL

Earth's Rotation and Straight and Level Flight

A perfect gyro maintains its spin axis with a constant direction in an inertial coordinate system. In general, such a gyro does not indicate a constant direction relative to a rotating earth or to an aircraft moving over the earth. In other words, to an observer in an earth-fixed or aircraft-fixed coordinate system it appears that the gyro is subject to some external (apparent) torque. If the gyro is to indicate the vertical, this apparent torque must be cancelled by an applied torque which differs from the apparent torque only in sign. Expressions for these torques are derived in the following paragraphs.

Consider the situation in which an airplane is in straight and level flight on course α (east of north) at latitude λ with constant speed v feet per second. With no loss in generality it is assumed that the airplane is flying tangent to the earth. An A-xyz coordinate system is defined so that the origin A is at the center of gravity of the gyro rotor in the airplane; the x-axis is tangent to the parallel of latitude at A and is positive eastward; the y-axis is tangent to the meridian at A and is positive northward; the z-axis is perpendicular to the earth at A and is positive upward.

The vector rotation, $\bar{\Omega}'$, of the A-xyz coordinate system is given by the component equations:

$$\left. \begin{aligned} \Omega'_x &= -\frac{v}{R} \cos \alpha, \\ \Omega'_y &= \omega \cos \lambda + \frac{v}{R} \sin \alpha, \text{ and} \\ \Omega'_z &= \omega \sin \lambda, \end{aligned} \right\} \quad (4)$$

where R is the radius of the earth (2.1×10^7 feet), and ω is the constant rotational speed of the earth (7.29×10^{-5} radians/second).

Suppose that the gyro is free of all torques including friction. In this situation the gyro maintains a constant direction in inertial space. To an observer fixed in the A-xyz coordinate system, the gyro appears to be subject to a rotation $-\bar{\Omega}'$. Therefore, the torque which cancels this motion is determined by $\bar{\Omega}'$ which Equations 4 give in component form.

For greater ease in visualization, Equations 4 are considered in two parts. First, let $v = 0$; that is, consider only the earth's rotation. Assume that the gyro is uncaged on the vertical; that is, the spin axis coincides with the z-axis. (If no torques are applied, the spin axis leaves the vertical in the direction of the negative x-axis.) A derivation similar to that given in Appendix A shows that the torque corresponding to Equations 4, with $v = 0$, is

$$\left. \begin{aligned} L_x &= I_z s \omega \cos \lambda, \text{ and} \\ L_y &= L_z = 0, \end{aligned} \right\} \quad (5)$$

where ω^2 terms have been dropped because ω^2 is negligible when compared with $s\omega$.

Under the scheme discussed in connection with Equations 3, no torque is applied as long as the gyro spin axis (indicated vertical) and the dynamic vertical are coincident. (In the present discussion the dynamic and static verticals are coincident.) Therefore, the gyro spin axis will deviate from the vertical sufficiently to generate the torque given by Equations 5. Obviously the system must be designed so that this deviation is not large enough to destroy the effectiveness of the gyro as an indicator of the vertical. A torque generated in accord with Equations 3 has its axis perpendicular to the gyro spin axis and in the plane determined by the spin axis and the dynamic vertical. This condition is satisfied also by the torque given by Equations 5 provided the spin axis is nearly coincident with the dynamic vertical. Under these conditions the torque generated in accord with Equations 3 satisfies the equality

$$I_z s \omega \cos \lambda = I_z s K \beta \frac{\pi}{180}$$

Hence, the gyro will come to rest with respect to the static vertical when

$$\omega \cos \lambda = K \beta \frac{\pi}{180}$$

The largest value of β will appear when $\lambda = 0$, where

$$\beta = 0.05^\circ, \text{ when } K = 1/12, \text{ and}$$

$$\beta = 0.25^\circ, \text{ when } K = 1/60.$$

K is determined by the value of β_1 in Equations 3 and the response rate of the gyro in regime (b). Therefore, the deviation of the gyro spin axis from the static vertical is small when the response rate of the gyro in regime (b) is large.

Now consider the effect of straight and level flight over a nonrotating earth at a constant speed of $v = 1000 \text{ ft./sec.}$ In this situation let $\omega = 0$ in Equations 4. Then the torque required to balance the effect of aircraft motion is

$$\left. \begin{aligned} L_x &= I_z s \frac{v}{R} \sin \alpha, \\ L_y &= I_z s \frac{v}{R} \cos \alpha, \text{ and} \\ L_z &= 0. \end{aligned} \right\} \quad (6)$$

Equations 6 may be replaced with the single torque

$$L_{fp} = I_z s \frac{v}{R}, \quad (7)$$

where $fp = \text{flight path.}$

Again assume that the gyro is uncaged with its spin axis on the static vertical. Because the spin axis leaves the vertical in the direction of the negative flight path the torque axis is in the plane determined by the dynamic vertical and the indicated vertical (gyro spin axis). Furthermore the torque axis is sufficiently near perpendicular to the indicated vertical for the appropriate one of Equations 3 to apply. That is,

$$I_z s \frac{v}{R} = I_z s K \beta \frac{\pi}{180},$$

whence

$$\beta = 0.033^\circ, \text{ when } K = 1/12, \text{ and}$$

$$\beta = 0.16^\circ, \text{ when } K = 1/60.$$

These values of β show the deviation of indicated vertical from static vertical (static and dynamic verticals are coincident) required to generate a torque sufficient to cancel the effects of straight and level flight. (Aircraft speeds considered in the remainder of this report lie in the 500-1000 ft/sec range.)

Coriolis Acceleration

In Appendix B it is shown that the angle between static and dynamic verticals because of Coriolis acceleration is (Equation B.15)

$$\epsilon_C = \frac{\omega v \sin \lambda}{16}.$$

For constant speeds ϵ_C is substantially constant for comparatively long periods of time. Therefore, the indicated vertical comes to rest at the angle ϵ_C away from the static vertical. This error varies from 0.25° at the geographic poles to 0° at the equator when the speed of the airplane is 1000 ft/sec. This error is discussed in connection with others in Chapter II.

Gyro Drift

The presence of bearing friction and the resulting gyro drift is one reason for applying correcting torques. Drift rates as low as 1° per hour appear to be attainable with comparative ease. Assume for the moment that gyro drift is the only disturbing element (that is, the dynamic and static verticals are coincident). An analysis similar to those given in the preceding paragraphs of this chapter shows that a 1° -per-hour drift rate is balanced by a deviation between indicated and static verticals of approximately 0.003° when $K = 1/12$, or 0.016° when $K = 1/60$. In practical application this probably means that the indicated vertical deviates from the static vertical only by the angle required to initiate a counter torque under regime (a). Throughout the remainder of this report the effects of gyro drift are considered negligible.

Airplane Maneuvers

In the preceding paragraphs of this chapter regime (c) has not been mentioned explicitly. The need for regime (c) is emphasized by sustained deviations from straight and level flight. Consider a perfectly banked turn through 180° and assume that $a = v^2/r$, where a is the radial acceleration and r is the radius of turn, throughout the deviation from straight and level flight. Suppose that regime (c) is absent. At the end of a 2g turn at 1000 ft/sec the indicated vertical is in error by approximately 8° when $K = 1/12$, or by 1.6° when $K = 1/60^*$. After the airplane returns to straight and level flight the indicated vertical returns to 0.1° from static vertical within 1.2 minutes when $K = 1/12$ or within 2.8 minutes when $K = 1/60$. The times required to return to 0.01° from static vertical are 1.6 minutes when $K = 1/12$ or 5 minutes when $K = 1/60$.

* As stated earlier in this report $K = 1/12$ or $K = 1/60$ when the erection rate of the gyro in regime (b) is 10° per minute or 2° per minute, respectively.

If a 180° turn is made at 2g and 500 ft/sec, or at 4g and 1000 ft/sec, the indicated vertical is in error by 4° when $K = 1/12$, or by 0.8° when $K = 1/60$. Upon return to straight and level flight these errors are reduced to 0.1° at the end of 0.8 minute when $K = 1/12$, or 2 minutes when $K = 1/60$; the errors are 0.01° at the end of 1.2 minutes when $K = 1/12$, or 4.4 minutes when $K = 1/60$.

Table I summarizes the discussion of the above two paragraphs.

TABLE I
Error in Indicated Vertical Caused by 180° Turn
(Regime (c) Absent)

Radial acceleration (g units)	Aircraft speed (ft/sec)	Error in indicated vertical at end of turn		Indicated vertical returns to (degrees error) at end of (minutes)		
		K = 1/12 (degrees)	K = 1/60 (degrees)	(degrees)	K = 1/12 (minutes)	K = 1/60 (minutes)
2	1000	8	1.6	{ 0.1 0.01	1.2 1.6	2.8 5.0
2 4	500 } 1000 }	4	0.8	{ 0.1 0.01	0.8 1.2	2.0 4.4

Times are measured from completion of turn.

These examples show the need for regime (c), particularly when the indicated vertical is used as part of the fuzing system or for navigation purposes during airplane maneuvers. When regime (c) is present, the error in the indicated vertical in the foregoing examples of maneuvers would be negligible provided the transition from straight and level flight to flight in a circle required only a small fraction of a minute.

Conditions under which regime (b) is in effect throughout a slow maneuver are of interest. Regime (c) is present but not activated. Such a condition is exemplified by a perfectly banked turn at approximately 0.17g radial acceleration. Turns of this type may be expected of bombers in formation as they maneuver for a bombing run. Under such conditions about 2.5 minutes are required for a 90° turn at 500 ft/sec. In this maneuver the angle between static and dynamic verticals is nearly 10° (β_2 of Equations 3). At the end of the maneuver the error in the indicated vertical is approximately 10° when $K = 1/12$, or 5° when $K = 1/60$. The time

UNCLASSIFIED

required for the indicated vertical to return to 0.1° from static vertical is 1.4 minutes when $K = 1/12$, or 4.5 minutes when $K = 1/60$. The time required to return to 0.01° is 1.8 minutes when $K = 1/12$, or 6.5 minutes when $K = 1/60$.

In the example of the preceding paragraph the indicated vertical is sufficiently in error to be of little use for several minutes. It appears that a possible solution would be provided by a choice of erection rate rather than a fixed erection rate in regime (b). That is, let $K = 1/60$ during the turn and then switch to $K = 1/12$ at the return to straight and level flight. However, the indicated vertical would still be in error by 5° at the end of the turn, and the indicated vertical would require approximately one minute to return to the static vertical. Hence, it appears advisable to provide a complete cutout so that no torque is applied during slow maneuvers.

CHAPTER V

ESTIMATES OF DIFFERENCES BETWEEN STATIC AND
DYNAMIC VERTICALS FOR SEVERAL AIRPLANES

Equations which express the vector difference, δ , between static and dynamic verticals during disturbances to straight and level flight are derived in Appendix B. In this chapter data for use in these equations are discussed and estimates of deviations between static and dynamic verticals are derived for several airplanes.

Available data concerning the motions of an airplane in a turbulent atmosphere were collected primarily for the purpose of determining dynamic loading and its implications for the design of airplanes. Hence, such data on airplane motions are usually restricted to the results of vertical acceleration measurements. One source⁵ includes data on angular accelerations and angular velocities for the B-45 with methods for estimating the motions of other aircraft therefrom. These data (Table II of this report) give the "maxima that would be expected in day-to-day operation of a B-45 at 15,000 ft. altitude, 450-mph indicated air-speed."⁵ According to Reference 6* disturbances of the magnitude shown in Table II (i. e., disturbances induced by gusts of approximately 9-ft/sec effective velocity) occur on the average once in 1000 miles of flight through clear air.

Correlation of Gust Frequency with Altitude

The references used here do not agree on the correlation of gust frequency with altitude. According to Reference 5 the values in Table II would be one-half to two-thirds as large for the same probability of occurrence at a 40,000-foot altitude. Reference 6 states that there is little difference in frequency of moderate gusts at low altitudes versus that at high altitudes. According to Reference 8 the frequency distribution of gust intensities is independent of altitude when gust intensity is expressed in terms of indicated velocity. (In general, these statements need be amended for altitudes near or above the tropopause. The average altitude of the tropopause is approximately 36,000 feet. Above the tropopause there is a marked decrease in atmospheric turbulence. Near the tropopause there is a decrease in the number of large gusts and marked increase in the number of smaller gusts.⁶) In this paper it is assumed that the probability of meeting a gust of given equivalent velocity is independent of altitude within the range considered.

* The significant information from Reference 6 is reproduced in Fig. 2 of Reference 7.

TABLE II

Motions of B-45C Due to Atmospheric Turbulence

Linear accelerations (g units)	Angular accelerations (rad/sec ²)	Angular velocities (rad/sec)
$\Delta n = 0.60$ (vertical, \ddot{z})	$\ddot{\psi} = 0.15$ (yaw)	$\dot{\psi} = 0.080$
$\Delta l = 0.10$ (lateral, \ddot{y})	$\ddot{\theta} = 0.30$ (pitch)	$\dot{\theta} = 0.015$
negligible (longitudinal, \ddot{x})	$\ddot{\phi} = 0.45$ (roll)	$\dot{\phi} = 0.170$

The maximum effective gust velocity U_e is approximately 9 ft/sec.

Aircraft Motions Through Atmospheric Turbulence

The air speeds used in this memorandum (Tables III and IV) were obtained from Division 5141 files. These are combat air speeds (true) at the altitudes shown in Table IV. To avoid the introduction of another variable, these air speeds are used at the lower altitude also (Table III). Only in the case of the B-36D (at 15,000 feet) does the tabulated air speed appear to be substantially above the proper value. However, this has no effect on the conclusions reached in this memorandum.

The application of the formulas of Reference 5 and the data of Table II gives the results in Tables III and IV.*

Values of x_{AP} and z_{AP} [†] are estimated from scale drawings on the assumption that the instrument is in the nose and in the plane of symmetry of the aircraft. These values appear in Table V.

* Because the computational procedure was set up for those aircraft listed in Tables III, IV and V before Reference 5 became available, and because the period of deviations from straight and level flight appears later to be of greater importance in determining the error in the indicated vertical, the B-45C does not appear in later computations.

[†] Coordinates of the vertical indicator when it is in the nose of the aircraft are x_{AP} (the distance forward from the aircraft center of gravity), y_{AP} (lateral distance from aircraft center line), and z_{AP} (the distance above or below the center line).

TABLE III

Estimates of Motions of Various Airplanes Due to Atmospheric Turbulence
(altitude 15,000 feet, effective gust velocity 9 ft/sec)

	<u>B-36D</u>	<u>B-47B</u>	<u>B-52</u>	<u>F-84F</u>	<u>F2H-2</u>
Air speed (mph, true)	395	560	594	633	530
<u>Linear accelerations (g units)</u>					
\ddot{z} (vertical)	0.36	0.30	0.43	0.41	0.42
\ddot{y} (lateral)	0.085	0.12	0.082	0.19	0.16
<u>Angular accelerations (rad/sec²)</u>					
$\ddot{\theta}$ (pitch)	0.097	0.082	0.074	0.39	0.73
$\ddot{\psi}$ (yaw)	0.056	0.15	0.068	0.79	0.55
$\ddot{\phi}$ (roll)	0.12	0.34	0.23	1.3	0.84
<u>Angular velocities (rad/sec)</u>					
$\dot{\theta}$ (pitch)	0.0069	0.0042	0.0035	0.018	0.039
$\dot{\psi}$ (yaw)	0.042	0.082	0.035	0.38	0.31
$\dot{\phi}$ (roll)	0.066	0.13	0.082	0.45	0.34

TABLE IV

Estimates of Motions of Various Airplanes Due to Atmospheric Turbulence
(effective gust velocity U_e is 9 ft/sec)

Airplane	<u>B-36D</u>	<u>B-47B</u>	<u>B-52</u>	<u>F-84F</u>	<u>F2H-2</u>
Altitude (ft)	25,000	35,000	35,000	35,000	35,000
<u>Linear accelerations (g units)</u>					
\ddot{z} (vertical)	0.30	0.21	0.30	0.29	0.28
\ddot{y} (lateral)	0.071	0.084	0.058	0.13	0.10
<u>Angular accelerations (rad/sec²)</u>					
$\ddot{\theta}$ (pitch)	0.068	0.040	0.036	0.19	0.36
$\ddot{\psi}$ (yaw)	0.039	0.075	0.034	0.39	0.27
$\ddot{\phi}$ (roll)	0.10	0.24	0.16	0.93	0.55
<u>Angular velocities (rad/sec)</u>					
$\dot{\theta}$ (pitch)	0.0058	0.0029	0.0025	0.012	0.027
$\dot{\psi}$ (yaw)	0.036	0.058	0.024	0.26	0.22
$\dot{\phi}$ (roll)	0.066	0.13	0.082	0.45	0.34

TABLE V

Coordinates of Vertical Indicator
in Nose of Aircraft
($y_{AP} = 0$)

Airplane	x_{AP} (ft)	z_{AP} (ft)
B-36D	+65	± 7
B-47B	+32	± 3
B-52	+41	± 4
F-84F	+13	± 1
F2H-2	+12	± 1

Angular Differences Between Dynamic and Static Verticals

The data of Tables III, IV, and V are substituted into equations B.8, B.9, and B.10 (Appendix B) which are added to produce the magnitude of the vector $\bar{\delta}$. In this evaluation algebraic signs are chosen arbitrarily (when possible) so as to amplify the angular difference, ϵ_{\max} , between the dynamic and static verticals to be expected in clear air. These values of ϵ_{\max} appear in Table VI. The probabilities are computed from the combat speed of the airplane and the 1000 miles average distance required to exceed $U_e = 9$ ft/sec effective gust velocity.

TABLE VI

Angular Deviation, ϵ_{\max} , of Dynamic Vertical from Static
Vertical with Probability of Occurrence
in Four Minutes of Flight
(instrument in nose of airplane)

Airplane	Altitude (ft)	Angular deviation, ϵ_{\max} (degrees)	Altitude (ft)	Angular deviation, ϵ_{\max} (degrees)	Probability (less than)
B-36D	15,000	27	25,000	17	0.03
B-47B	15,000	27	35,000	13	0.04
B-52	15,000	23	35,000	11	0.04
F-84F	15,000	57	35,000	29	0.04
F2H-2	15,000	54	35,000	20	0.04

The "less than" of the probability column of Table VI is based upon observations that maximum linear accelerations and maximum angular accelerations rarely occur simultaneously (as is assumed in deriving the values of ϵ_{\max}). Furthermore, the algebraic signs

applied to the quantities of Table III are chosen in an arbitrary (but consistent) fashion designed to give high values of ϵ_{\max} , and the periods of pitch, roll, and yaw are not necessarily equal as assumed in computing these values of ϵ_{\max} .

For an instrument at the center of gravity of the airplane, angular accelerations and velocities do not enter the determination of the vector difference between dynamic and static verticals. In this case the deviations of Table VI become those of Table VII.

TABLE VII

Angular Deviation, ϵ_{\max} of Dynamic Vertical from Static Vertical for Instrument at Center of Gravity of Airplane

Airplane	Altitude (ft)	ϵ_{\max} (degrees)	Altitude (ft)	ϵ_{\max} (degrees)	Probability
B-36D	15,000	7	25,000	6	0.03
B-47B	15,000	9	35,000	6	0.04
B-52	15,000	8	35,000	5	0.04
F-84F	15,000	16	35,000	10	0.04
F2H-2	15,000	18	35,000	8	0.04

In Table VII the probability estimates are more accurate than those in Table VI because angular motions with their attendant uncertainties are not included in the determination of ϵ_{\max} .

The effects of flexible wings upon the motions of an airplane in a gust are not well known and hence do not appear in the foregoing estimates of ϵ_{\max} . However, both flexibility and sweepback are known to be reducing factors.⁸ Differences in piloting are not specifically mentioned in this analysis since little is known of these effects. However, measurements made under operating conditions (as were those of Reference 5) include piloting effects for the pilots involved.

The data presented in Tables II, III, IV, VI, and VII represent disturbances to straight and level flight which, on the average, are equaled or exceeded once in approximately 1000 miles of flight. For such disturbances the effective gust velocity, U_g , is at least 9 ft/sec. The probability of meeting a disturbance of such magnitude during a flight time of four minutes is small (Tables VI and VII). (Four minutes is assumed to be sufficient time for aligning the vertical reference in the weapon and for calibrating and activating the vertical distance meter.) A question naturally arises concerning the disturbances that may be

expected with high probability during a four-minute time interval. Disturbances to straight and level flight for which the effective gust velocity is at least 3 ft/sec are expected on the average once in 10 miles of flight*.⁶ Because the airplanes used as examples herein fly further than 10 miles in the arbitrary four-minute period, the probability of experiencing a gust whose effective velocity is at least 3 ft/sec is approximately one.

Data comparable with those of Table II but for $U_e \geq 3$ ft/sec apparently are not available. It is therefore necessary to extrapolate from Tables III and IV for such disturbances. The gust formula (see Reference 7, page 6, or Reference 8, page 4, for example) indicate that linear accelerations vary directly with the effective gust velocity. Available data (Reference 8, page 58) indicate that acceleration in pitch varies directly with vertical acceleration and hence with effective gust velocity. Available data (Reference 8, Table V) also indicate that no strong correlation exists between gust velocity and acceleration in roll. Apparently no data are available concerning correlation between gust velocity and acceleration in yaw. It is therefore necessary to assume that acceleration in yaw varies directly with gust velocity as appears to be true of pitch accelerations. Data comparable with those of Tables VI and VII, except for $U_e = 3$ ft/sec, appear in Table VIII.

TABLE VIII

Estimate of Angular Deviation, ϵ_{\max} , of Dynamic Vertical from
Static Vertical Because of Atmospheric Turbulence
(effective gust velocity, $U_e = 3$ ft/sec)

Airplane	Altitude (ft)	ϵ_{\max} (degrees)		Altitude (ft)	ϵ_{\max} (degrees)	
B-36D	15,000	5*	2**	25,000	4*	2**
B-47B	15,000	5*	2**	35,000	3*	1**
B-52	15,000	6*	2**	35,000	4*	2**
F-84F	15,000	13*	4**	35,000	7*	3**
F2H-2	15,000	10*	4**	35,000	5*	2**

* Instrument in nose of airplane
** Instrument at center of gravity of airplane

* The significant information from Reference 6 is reproduced in Fig. 2 of Reference 7.

Examination of Equations B. 8, B. 9, and B. 10 (in Appendix B) with Tables III, IV, and V in mind shows that (for an instrument in the nose of the aircraft) angular velocities contribute little to the magnitude of ϵ_{\max} (angular deviation of dynamic vertical from static vertical). By far the largest contribution to ϵ_{\max} (as a result of angular motion) is made by acceleration in yaw. Therefore, the significant assumption underlying the derivation of values of ϵ_{\max} of Table VIII is that yaw acceleration varies directly with gust velocity. Obviously this assumption has no effect when the instrument is at the center of gravity of the airplane.

On the basis of assumptions discussed in the two preceding paragraphs the values of ϵ_{\max} in Table VIII (for an instrument in the nose of the airplane) are obtained by using the entries (except those for air speed) of Tables III and IV divided by three.

In Chapter VI $\epsilon_{\max} = 2^{\circ}$, 7° , and 27° are taken as representative in the estimation of errors to be expected in the indicated vertical because of atmospheric disturbances in clear air.

UNCLASSIFIED

CHAPTER VI

ESTIMATES OF ERRORS IN INDICATED VERTICAL
BECAUSE OF ATMOSPHERIC DISTURBANCES

Estimates of the deviations, γ , of indicated vertical from static vertical (errors in the indicated vertical) are derived in this chapter.

Because the timewise history of disturbances to straight and level flight of an aircraft is not known, it is necessary to assume that the three verticals are coplanar. Then $\beta = \epsilon - \gamma$, where ϵ and γ are measured from the static vertical to the dynamic vertical and to the indicated vertical, respectively; β is measured from the indicated vertical to the dynamic vertical. It should be emphasized that neither γ nor ϵ is a measure of aircraft attitude. The three verticals are assumed to be coincident at time $t = 0$ when the disturbed flight begins. For purposes of illustration the direction of first motion of indicated and dynamic verticals away from static vertical is defined to be positive.

Method of Applying Torques

The response rate of the gyro is controlled under three regimes:

$$\left. \begin{array}{ll} \text{(a)} & \dot{\gamma} = K(\epsilon - \gamma) \text{ when } 0 \leq |\epsilon - \gamma| \leq 2^\circ, \\ \text{(b)} & \dot{\gamma} = +2K \text{ when } 2^\circ \leq |\epsilon - \gamma| \leq 10^\circ, \text{ and} \\ \text{(c)} & \dot{\gamma} = 0 \text{ when } 10^\circ < |\epsilon - \gamma|. \end{array} \right\} \quad (8)$$

Note that $\dot{\gamma}$ is measured in degrees per second. Equations 8 are equivalent to Equations 3; $K = 1/12$ when $\dot{\gamma} = 1/6^\circ$ per second (10° per minute), and $K = 1/60$ when $\dot{\gamma} = 1/30^\circ$ per second (2° per minute) in regime (b); $\dot{\gamma}$ is positive when $\epsilon > \gamma$ and negative when $\epsilon < \gamma$ in both regimes (a) and (b). Only situations in which $K = 1/12$ are illustrated. For purposes of illustration in this chapter the times when one regime surrenders to another are determined graphically.

Mathematical Models

The variation in ϵ is represented by two different equations in order to bracket the actual situation. The equation

$$\epsilon = \epsilon_{\max} \sin \frac{n\pi t}{5} \quad (9)$$

certainly presents one extreme in the sense that the variation in ϵ is not damped. In Equation 9, n is 1 or 2 and ϵ_{\max} is 2° , 7° , or 27° as indicated at the end of Chapter VI. The following equation

$$\epsilon = H e^{-\frac{3nt}{10}} \sin \frac{n\pi t}{5} \quad (10)$$

(where H is a constant whose value depends upon ϵ_{\max}) represents the other extreme in that the variation in ϵ is damped out rapidly. In Equation 10, H is 27/7, 27/2, or 52. These values of H give values of ϵ_{\max} which closely approximate 2° , 7° , or 27° , respectively. The smallest of these amplitudes, 2° , is representative of values of ϵ_{\max} which will be exceeded with a high probability during a few minutes of flight (Table VIII); 7° is representative of values which will be exceeded frequently in the nose of the aircraft (Table VIII) but rarely at the center of gravity of the aircraft (Table VII); 27° is representative of values of ϵ_{\max} rarely exceeded in the nose of the aircraft (Table VI). When ϵ_{\max} substantially exceeds the 10° limit which divides regimes (b) and (c), the period of the variation in ϵ becomes dominant in determining the error in the indicated vertical. Hence, the largest values of ϵ_{\max} in Table VI are not used in this chapter.

Periods of angular motion of aircraft usually lie between two and ten seconds. Periods of five and ten seconds, $n = 2$ and 1, respectively, in each of Equations 9 and 10, are used in this chapter. For shorter periods the error in the indicated vertical becomes negligible under the conditions of this analysis.

The solution of the differential equation defining regime (a) gives

$$\gamma = \frac{K\epsilon_{\max}}{K^2 + \left(\frac{n\pi}{5}\right)^2} \left(K \sin \frac{n\pi t}{5} - \frac{n\pi}{5} \cos \frac{n\pi t}{5} \right) + C e^{-Kt}, \quad (11)$$

when ϵ is determined by Equation 9, or

$$\gamma = \frac{K H e^{-\frac{3nt}{10}}}{\left(K - \frac{3n}{10}\right)^2 + \left(\frac{n\pi}{5}\right)^2} \left[\left(K - \frac{3n}{10}\right) \sin \frac{n\pi t}{5} - \frac{n\pi}{5} \cos \frac{n\pi t}{5} \right] + C e^{-Kt}, \quad (12)$$

when ϵ is determined by Equation 10. C , a constant of integration, is determined when a pair of corresponding values of γ and t are given.

Errors in Indicated Vertical Because of Gusts

Figure 3 illustrates the variation in both ϵ and γ when $K = 1/12$ and c is given by Equation 9 with $n = 1$. In Fig. 3A only regime (a) is in operation. The maximum error in the indicated vertical, γ , is approximately 0.4° . As time increases, γ approaches a sinusoidal variation with amplitude approximately 0.25° . If the period of ϵ is five seconds ($n = 2$), then the maximum error in the indicated vertical is approximately 0.25° ; γ eventually becomes sinusoidal with amplitude approximately 0.15° .

If $K = 1/60$ but all other conditions of Fig. 3A apply, the error in the indicated vertical does not exceed 0.1° .

In Fig. 3B the maximum error in the indicated vertical is approximately 0.7° . If the period is five seconds ($n = 2$), the maximum error is approximately 0.4° .

If $K = 1/60$ but all other conditions of Fig. 3B apply, then γ will not exceed 0.17° .

In Fig. 3C regime (c) is in operation throughout most of the cycle. In this situation the maximum error in the indicated vertical is approximately 0.2° . If the period of ϵ is five seconds, this maximum error is approximately 0.1° .

If $K = 1/60$ but all other conditions of Fig. 3C apply, then γ does not exceed 0.05° .

As far as maximum values of γ are concerned the preceding discussion of Figs. 3A and 3B applies to Figs. 4A and 4B for either value of K and will not be repeated. The most obvious difference between the parts of Figs. 3 and 4 is that ϵ takes both positive and negative values in Figs. 3A and 3B but never becomes negative (even for $t > 10$ seconds) in Figs. 4A and 4B.

In Fig. 4C the maximum absolute value of γ , approximately 0.5° , appears near the end of the first ten-second cycle. After approximately seven seconds γ remains negative. If the period is five seconds ($n = 2$), the maximum absolute value of γ is approximately 0.2° .

If $K = 1/60$ in Fig. 4C, but all other conditions remain the same, then γ is approximately 0.1° at its maximum absolute value.

The results discussed in the preceding paragraphs are summarized in Table IX.

UNCLASSIFIED

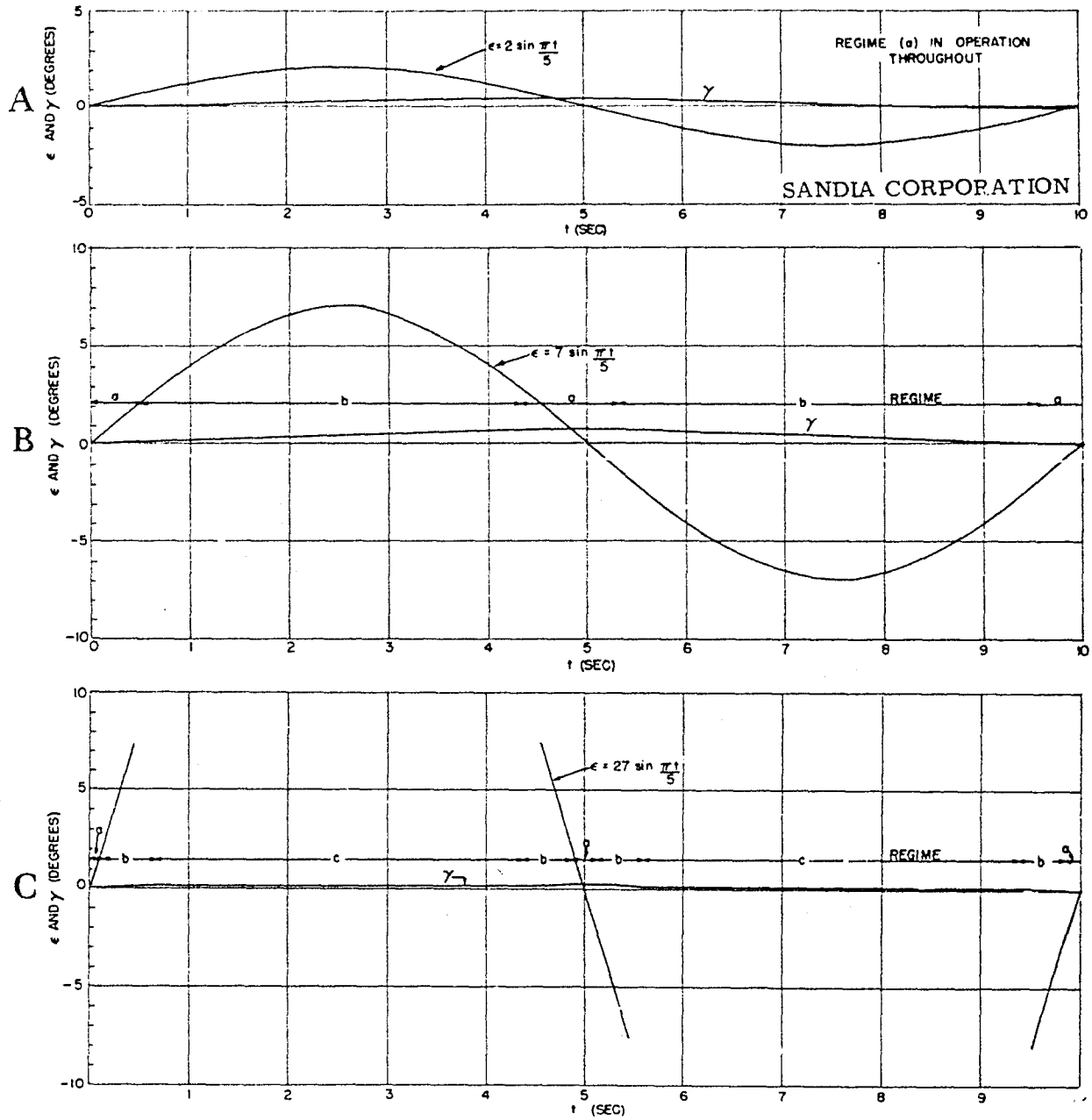


Fig. 3 -- Error in indicated vertical, γ , versus time when angle ϵ between static vertical and dynamic vertical is assumed to be given by sine function shown

See page 31 for definition of regimes (a), (b), and (c). Gyro erection rate is 10 degrees per minute in regime (b).

UNCLASSIFIED

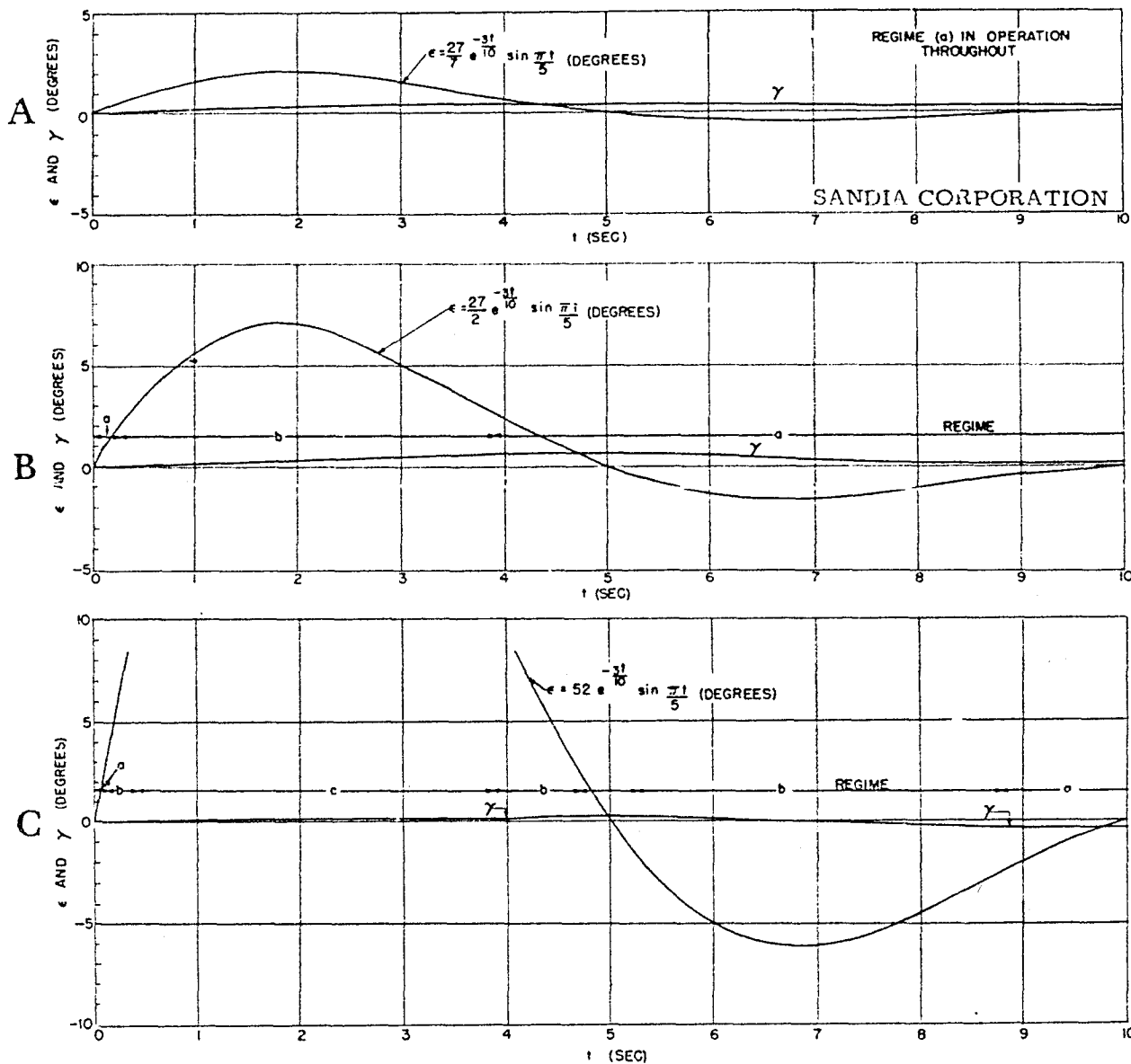


Fig. 4 -- Error in indicated vertical, γ , versus time when angle ϵ between static vertical and dynamic vertical is assumed to be given by damped sine function shown

See page 31 for definition of regimes (a), (b), and (c). Gyro erection rate is 10 degrees per minute in regime (b).

TABLE IX

Summary of Errors in Indicated Vertical as Determined from Figs. 3 and 4

Maximum angle between static and dynamic verticals (ϵ_{max} , degrees)	Period of variation in ϵ (seconds)	Variation in ϵ		Maximum error in indicated vertical (degrees)	
		Damped	Undamped	Response rate of gyro	
				$10^\circ/\text{min}$	$2^\circ/\text{min}$
2	10		x	0.4	0.1
2	5		x	0.25	<0.1
7	10		x	0.7	<0.2
7	5		x	0.4	<0.1
27	10		x	0.2	<0.05
27	5		x	0.1	<0.05
(When ϵ_{max} is 2° or 7° and the variation in ϵ is damped as in Equation 10, the results are essentially the same as above.)					
27	10	x		0.5	0.1
27	5	x		0.2	<0.1

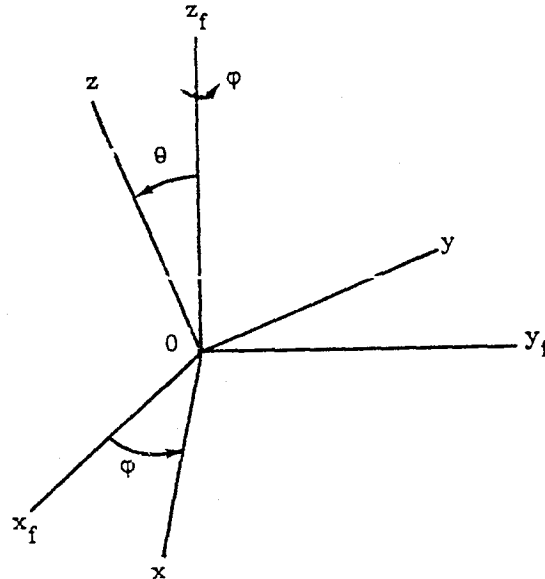
The conclusions of this study are presented at the end of Chapter II.

R. L. CALVERT - 5131

Case No. 418.01
November 4, 1955

APPENDIX A
FUNDAMENTALS OF GYROSCOPE THEORY

For the development of fundamental equations of gyroscope theory* (Equations A.1-A.6 of this appendix) two rectangular coordinate systems are defined. The coordinate system $0-x_f y_f z_f$ is fixed in inertial space with the center of gravity of the gyro rotor at 0. (See Fig. 2.) The coordinate system $0-xyz$ has the spin axis of the gyro as z -axis; the x -axis is the



$0z$ is the spin axis of the gyro
 $0y$ is in the $0zz_f$ plane
 $0x$ is in the $0x_f y_f$ plane

Fig. 2 -- Two rectangular coordinate systems
(repeated from page 17)

intersection of the $0x_f y_f$ plane and the plane perpendicular to $0z$ at 0; the y -axis is in the $0zz_f$ plane and completes a right-handed system. Because the gyro rotor is essentially a solid of revolution about the z -axis and the $0xy$ plane is perpendicular to this axis, moments of inertia about the x - and y -axes are equal; i. e.,

$$I_x = I_y.$$

Let θ be the angle $z0z_f$, and ϕ be the angle $x0x_f$.

* Comparable derivations may be found in texts on physical or theoretical mechanics.

Suppose the gyro is in motion as the result of an applied torque. This motion is represented by the angular velocity vector $\bar{\Omega}$ which has the component form

$$\left. \begin{aligned} \Omega_x &= \dot{\theta}, \\ \Omega_y &= \dot{\phi} \sin \theta, \text{ and} \\ \Omega_z &= \dot{\phi} \cos \theta \end{aligned} \right\} \quad (A.1)$$

with respect to the 0-xyz coordinate system.

The vector angular momentum is

$$\bar{B} = iI_x \dot{\theta} + jI_x \dot{\phi} \sin \theta + kI_z (s + \dot{\phi} \cos \theta), \quad (A.2)$$

where s is the spin velocity of the rotor and is assumed to be constant.

The applied torque is the time rate of change of the angular momentum. Hence

$$\bar{L} = \dot{\bar{B}}, \quad (A.3)$$

or

$$\begin{aligned} \bar{L} &= iI_x \ddot{\theta} + jI_x (\ddot{\phi} \sin \theta + \dot{\phi} \dot{\theta} \cos \theta) + kI_z (\dot{\phi} \cos \theta - \dot{\phi} \dot{\theta} \sin \theta) \\ &+ \begin{vmatrix} i & j & k \\ \dot{\theta} & \dot{\phi} \sin \theta & \dot{\phi} \cos \theta \\ I_x \dot{\theta} & I_x \dot{\phi} \sin \theta & I_z (s + \dot{\phi} \cos \theta) \end{vmatrix}^* \end{aligned} \quad (A.4)$$

In component form Equation A. 4 becomes

$$\left. \begin{aligned} L_x &= I_x (\ddot{\theta} - \dot{\phi}^2 \sin \theta \cos \theta) + I_z (s + \dot{\phi} \cos \theta) \dot{\phi} \sin \theta, \\ L_y &= I_x (\ddot{\phi} \sin \theta + 2\dot{\phi} \dot{\theta} \cos \theta) - I_z \dot{\theta} (s + \dot{\phi} \cos \theta), \text{ and} \\ L_z &= I_z (\dot{\phi} \cos \theta - \dot{\phi} \dot{\theta} \sin \theta). \end{aligned} \right\} \quad (A.5)$$

Equations A. 5 display the applied torque in terms of the gyro motions produced thereby. Applications of Equations A. 5 appeared in Chapters III and IV of this memorandum. For the purpose of this memorandum only terms in s are significant. Hence, Equations A. 5 are used in a form comparable with the following:

$$L_x = I_z s \dot{\phi} \sin \theta, \quad L_y = -I_z \dot{\theta} s, \quad \text{and } L_z = 0 \quad (A.6)$$

* The determinant of Equation A. 4 is a convenient form for expressing the terms arising from di/dt , dj/dt , and dk/dt .

APPENDIX B

DIFFERENCE BETWEEN DYNAMIC VERTICAL AND STATIC
VERTICAL IN AN AIRPLANE*

In this appendix expressions for the vector difference between dynamic and static verticals are derived. Coriolis acceleration, which appears in these derivations, is discussed also.

Consider the following three-dimensional rectangular coordinate systems:

- Origin at I, an inertial system;
- Origin at E (the center of the earth), and fixed in the earth
- Origin at S (a point on the earth's surface), and fixed on the earth; and
- Origin at A (the CG of the airplane), and fixed in the airplane.

P is the CG of the instrument or the point of support of a sensitive element of the instrument, whichever applies. Since the linear acceleration of the earth's center is negligible (of the order of 0.0005g), origins I and E may be considered coincident. Coordinate systems E and S are mutually nonrotating.

The following notation is used:

\bar{R}_{IE} = the position vector of point E in the I coordinate system, and

$\bar{\omega}_{IE}$ = the angular velocity vector of system E with respect to system I, etc., for other coordinate systems. The bar indicates vector quantities except where unit vectors i, j, and k are used.

In text books on physical mechanics the following equation is derived:

$$\ddot{\bar{R}}_{IP} = \ddot{\bar{R}}_{IE} + \ddot{\bar{R}}_{EP} + 2\bar{\omega}_{IE} \times \dot{\bar{R}}_{EP} + \dot{\bar{\omega}}_{IE} \times \bar{R}_{EP} + \bar{\omega}_{IE} \times (\bar{\omega}_{IE} \times \bar{R}_{EP}), \quad (\text{B.1})$$

where

$\ddot{\bar{R}}_{IP}$ = the acceleration of point P with respect to coordinate system I,

* The method used in this appendix is suggested by Reference 9.

$\ddot{\bar{R}}_{IE}$ = the acceleration of origin E with respect to coordinate system I (0 in this application),

$\ddot{\bar{R}}_{EP}$ = the acceleration of point P with respect to coordinate system E,

$2\bar{\omega}_{IE} \times \dot{\bar{R}}_{EP}$ = the acceleration of Coriolis due to rotation of system E with respect to system I,

$\dot{\bar{\omega}}_{IE} \times \bar{R}_{EP}$ = the acceleration of point P due to angular acceleration of system E with respect to system I, and

$\bar{\omega}_{IE} \times (\bar{\omega}_{IE} \times \bar{R}_{EP})$ = centripetal acceleration due to rotation of system E with respect to system I.

In Equation B.1 the $\dot{\bar{\omega}}_{IE}$ term is negligible.

For systems E and S, where $\bar{\omega}_{ES} = 0$ and $\ddot{\bar{R}}_{ES} = 0$,

$$\ddot{\bar{R}}_{EP} = \ddot{\bar{R}}_{SP}. \quad (\text{B.2})$$

To obtain the effects of the motions of system A with respect to system S, Equation B.1 may be written as

$$\ddot{\bar{R}}_{SP} = \ddot{\bar{R}}_{SA} + \ddot{\bar{R}}_{AP} + 2\bar{\omega}_{SA} \times \dot{\bar{R}}_{AP} + \dot{\bar{\omega}}_{SA} \times \bar{R}_{AP} + \bar{\omega}_{SA} \times (\bar{\omega}_{SA} \times \bar{R}_{AP}), \quad (\text{B.3})$$

where $\ddot{\bar{R}}_{AP} = \dot{\bar{R}}_{AP} = 0$, since the point P is fixed in the airplane.

Substitution from Equations B.2 and B.3 into Equation B.1 results in

$$\ddot{\bar{R}}_{IP} = \ddot{\bar{R}}_{SA} + 2\bar{\omega}_{IE} \times \dot{\bar{R}}_{EP} + \bar{\omega}_{IE} \times (\bar{\omega}_{IE} \times \bar{R}_{EP}) + \dot{\bar{\omega}}_{SA} \times \bar{R}_{AP} + \bar{\omega}_{SA} \times (\bar{\omega}_{SA} \times \bar{R}_{AP}). \quad (\text{B.4})$$

Equation B.4 expresses the motion of point P in terms of the motions of the various coordinate systems. Before Equation B.4 can be of use the acceleration due to universal gravitational attraction must be introduced.

The acceleration of gravity as measured by a plumb bob includes the universe gravitational acceleration and the centripetal acceleration due to the earth's rotation. That is,

$$\bar{g} = \bar{\omega}_{IE} \times (\bar{\omega}_{IE} \times \bar{R}_{EP}) + \frac{\bar{GM}}{R_{EP}^2}, \quad (\text{B.5})$$

where M is the mass of the earth. Introducing this change into Equation B.4 results in

$$\ddot{\bar{R}}_{IP} = \ddot{\bar{R}}_{SA} + 2\bar{\omega}_{IE} \times \dot{\bar{R}}_{EP} + \dot{\bar{\omega}}_{SA} \times \bar{R}_{AP} + \bar{\omega}_{SA} \times (\bar{\omega}_{SA} \times \bar{R}_{AP}) + \bar{g}, \quad (\text{B.6})$$

which describes the motion of point P in an inertial system.

The $2\bar{\omega}_{IE} \times \dot{\bar{R}}_{EP}$ term of Equation B.6 is the Coriolis acceleration which is discussed in a later section of this appendix. The remaining three of the first four terms on the right of Equation B.6 represent accelerations arising from disturbances to straight and level flight (e.g., atmospheric turbulence and piloting effects). Let $\bar{\delta}$ represent the vector sum of these three terms; that is,

$$\bar{\delta} = \ddot{\bar{R}}_{SA} + \dot{\bar{\omega}}_{SA} \times \bar{R}_{AP} + \bar{\omega}_{SA} \times (\bar{\omega}_{SA} \times \bar{R}_{AP}). \quad (\text{B.7})$$

Actually $\bar{\delta}$ is the acceleration acting at the point P and $-\bar{\delta}$ enters the definition of the dynamic vertical. However, $\bar{\delta}$ has a random direction. Therefore, the application of Equation B.7 in this report emphasizes ϵ , the angle between \bar{g} and $\bar{g} - \bar{\delta}$. Hence no distinction need be made between $\bar{\delta}$ and $-\bar{\delta}$.

For any bombing or calibration run the origin of the S coordinate system is fixed on the earth directly below point A at the beginning of the run. Flight over a spherical earth will contribute to $\bar{\omega}_{SA}$. However, this contribution was discussed in Chapter IV.

In the A coordinate system the x_A -axis is parallel to the longitudinal axis of the airplane and is positive forward; the Ax_Az_A plane is the plane of symmetry of the craft with z_A positive upward; the y_A -axis is positive to the left. Angular motions of the A -coordinate system with respect to the same system are θ = pitch (around the y_A -axis), ϕ = roll (around the x_A -axis), and ψ = yaw (around the z_A -axis) with positive directions chosen to make the system right-handed.

In component form the terms of Equation B.7 become

$$\ddot{\bar{R}}_{SA} = i_A \ddot{x}_{AA} + j_A \ddot{y}_{AA} + k_A \ddot{z}_{AA}, \quad (\text{B.8})$$

$$\dot{\bar{\omega}}_{SA} \times \bar{R}_{AP} = i_A (z_{AP} \ddot{\theta} - y_{AP} \ddot{\psi}) + j_A (x_{AP} \ddot{\psi} - z_{AP} \dot{\phi}) + k_A (y_{AP} \dot{\phi} - x_{AP} \dot{\theta}) \quad (\text{B.9})$$

UNCLASSIFIED

and

$$\begin{aligned}
\bar{\omega}_{SA} \times (\bar{\omega}_{SA} \times \bar{R}_{AP}) = & i_A(\dot{\theta}\dot{\phi}y_{AP} - \dot{\theta}^2x_{AP} - \dot{\psi}^2x_{AP} + \dot{\psi}\dot{\phi}z_{AP}) \\
& + j_A(\dot{\psi}\dot{\theta}z_{AP} - \dot{\psi}^2y_{AP} - \dot{\phi}^2y_{AP} + \dot{\psi}\dot{\theta}x_{AP}) \\
& + k_A(\dot{\phi}\dot{\psi}x_{AP} - \dot{\phi}^2z_{AP} - \dot{\theta}^2z_{AP} + \dot{\psi}\dot{\theta}y_{AP}). \tag{B.10}
\end{aligned}$$

These equations were applied in Chapter V.

Coriolis Acceleration

The Coriolis acceleration term of Equations B.1 and B.6 is $\bar{a}_C = 2\bar{\omega}_{IE} \times \dot{\bar{R}}_{EP}$. Because the E and S coordinate systems are not mutually revolving, $\bar{a}_C = 2\bar{\omega}_{IS} \times \dot{\bar{R}}_{SP}$. For the purpose of this study the dynamic vertical is the direction defined by the resultant of $-\bar{a}_C$ and \bar{g} . Hence, $-\bar{a}_C$ is used in this section.

At the beginning of a straight and level calibration run let the S coordinate system be fixed so that the origin, S, is on the surface of the earth below the airplane. The z_S axis is perpendicular to the plane of the horizon and is positive upward. The x_S axis is tangent to the latitude circle at S and is positive eastward. The y_S axis is tangent to the meridian at S and is positive northward.

Let S be at latitude λ . Then

$$\bar{\omega}_{IS} = j_S\omega \cos \lambda + k_S\omega \sin \lambda, \tag{B.11}$$

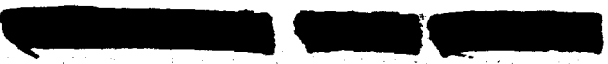
where ω is the rotational speed of the earth (7.29×10^{-5} rad/second). Let (x_S, y_S, z_S) be the coordinates of point P.

Then

$$\dot{\bar{R}}_{SP} = i_S\dot{x}_S + j_S\dot{y}_S + k_S\dot{z}_S, \tag{B.12}$$

and

$$-\bar{a}_C = -2\omega \begin{vmatrix} i_S & j_S & k_S \\ 0 & \cos \lambda & \sin \lambda \\ \dot{x}_S & \dot{y}_S & \dot{z}_S \end{vmatrix},$$



or

$$-\bar{a}_C = -2\omega \left[i_S(\dot{z}_S \cos \lambda - \dot{y}_S \sin \lambda) + j_S \dot{x}_S \sin \lambda - k_S \dot{x}_S \cos \lambda \right]. \quad (\text{B.13})$$

For an airplane flying straight and level on course α (east of north) at speed v

$$\dot{x}_S = v \sin \alpha, \quad \dot{y}_S = v \cos \alpha, \quad \text{and} \quad \dot{z}_S = 0.$$

Substitution into Equation B.13 and the separation of $-\bar{a}_C$ into horizontal and vertical components gives

$$\left. \begin{aligned} -\bar{a}_{CH} &= 2\omega v \sin \lambda (i_S \cos \alpha - j_S \sin \alpha) \text{ and} \\ -\bar{a}_{CV} &= 2\omega v \cos \lambda (k_S \sin \alpha). \end{aligned} \right\} \quad (\text{B.14})$$

The $-\bar{a}_{CH}$ vector extends in the direction $\alpha + 90^\circ$ in north latitudes and in the direction $\alpha - 90^\circ$ in south latitudes, and its magnitude is $2\omega v \sin \lambda$.

The difference between static and dynamic verticals when no acceleration other than that of Coriolis is present is

$$\epsilon_C = \arctan \frac{2\omega v \sin \lambda}{g + 2\omega v \sin \alpha \cos \lambda}.$$

Because $2\omega v$ is numerically small with respect to g , the following approximation is sufficient for the purpose of this report:

$$\epsilon_C \approx \frac{\omega v \sin \lambda}{16} \text{ (radians)}. \quad (\text{B.15})$$

LIST OF REFERENCES

1. Buell, C. E., 5132, Time-of-Fall Fuzing System Feasibility for Strategic Bombing, SC-2439(TR), August 1952.
2. Hatfield, T. N., 5131, Remarks on the Use of a Double-Integrating Accelerometer in Vertical Distance Fuzing of an Airburst Weapon, SC-2473(TR), August 22, 1952.
3. Bridges, A. P., 5143, Preliminary Analysis Regarding the Use of Inertial Distance Meters to Fuze an Air Burst Weapon, Working Paper, Ref. Sym: 5143(13), May 26, 1952.
4. Deflections of the Vertical at High Altitudes, Army Map Service Tech. Report, August 31, 1951, DA-Q-35.
5. Letter, Rhode, Richard V., NACA, to Brodsky, R. F., 5141, April 23, 1952.
6. Hislop, G. S., and Davies, D. M., Final Report of Clear Air Gust Research Project, British European Airways Corporation, June 1951, RSD Report No. 15.
7. Lane, F. O., Vertical Velocities Induced in Airplanes by Atmospheric Turbulence, SC-1952(TR), August 17, 1951.
8. Donely, Philip, Summary of Information Relating to Gust Loads on Airplanes, NACA Technical Note 1976, Washington, D. C., November 1949.
9. Wigley, Walter, An Investigation of Methods Available for Indicating the Direction of the Vertical from Moving Bases, D.Sc. Thesis, MIT, 1934.

UNCLASSIFIED

$$\ddot{\bar{R}}_{HQ} = \cancel{\ddot{\bar{R}}_{MP}} + \cancel{\ddot{\bar{R}}_{PQ}} + 2\cancel{\bar{\omega}_{MP}} \times \dot{\bar{R}}_{PQ} + \dot{\bar{\omega}}_{MP} \times \bar{R}_{PQ} + \bar{\omega}_{MP} \times (\bar{\omega}_{MP} \times \bar{R}_{PQ})$$

$$\ddot{\bar{R}}_{SQ} = \ddot{\bar{R}}_{SM} + \ddot{\bar{R}}_{MQ} + 2\bar{\omega}_{SM} \times \dot{\bar{R}}_{MQ} + \dot{\bar{\omega}}_{SM} \times \bar{R}_{MQ} + \bar{\omega}_{SM} \times (\bar{\omega}_{SM} \times \bar{R}_{MQ})$$

$$\ddot{\bar{R}}_{IQ} = \cancel{\ddot{\bar{R}}_{IS}} + \ddot{\bar{R}}_{SQ} + 2\bar{\omega}_{IS} \times \dot{\bar{R}}_{SQ} + \dot{\bar{\omega}}_{IS} \times \bar{R}_{SQ} + \bar{\omega}_{IS} \times (\bar{\omega}_{IS} \times \bar{R}_{SQ})$$

$$\ddot{\bar{R}}_{IP} = \cancel{\ddot{\bar{R}}_{IS}} + \ddot{\bar{R}}_{SP} + 2\bar{\omega}_{IS} \times \dot{\bar{R}}_{SP} + \dot{\bar{\omega}}_{IS} \times \bar{R}_{SP} + \bar{\omega}_{IS} \times (\bar{\omega}_{IS} \times \bar{R}_{SP})$$

$$\ddot{\bar{R}}_{SP} = \ddot{\bar{R}}_{SM} + \cancel{\ddot{\bar{R}}_{MP}} + 2\bar{\omega}_{SM} \times \dot{\bar{R}}_{MP} + \dot{\bar{\omega}}_{SM} \times \bar{R}_{MP} + \bar{\omega}_{SM} \times (\bar{\omega}_{SM} \times \bar{R}_{MP})$$

$$\begin{aligned} \ddot{\bar{R}}_{IP} &= \ddot{\bar{R}}_{SM} + 2\bar{\omega}_{IS} \times \dot{\bar{R}}_{SP} + \bar{\omega}_{IS} \times (\bar{\omega}_{IS} \times \bar{R}_{SP}) \\ &\quad + \dot{\bar{\omega}}_{SM} \times \bar{R}_{MP} + \bar{\omega}_{SM} \times (\bar{\omega}_{SM} \times \bar{R}_{MP}) \end{aligned}$$